Electronic Supplementary Information

Green Synthesis of AgI Nanoparticle–Functionalized Reduced Graphene Oxide Aerogels with Enhanced Catalytic Performance and Facile Recycling

D. Amaranatha Reddy, Jiha Choi, Seunghee Lee, Rory Ma, and Tae Kyu Kim[*]

Department of Chemistry and Chemical Institute for Functional Materials, Pusan National University, Busan 609-735, Republic of Korea

*E-mail address: tkkim@pusan.ac.kr

Experimental and characterizations

The Pure AgI and AgI-RGAs (1, 2, 3, 4, and 5 mg·mL^{-1} of GO) nanocomposites were chemically synthesized using an *in situ* ultrasound-assisted method. The reactants were silver nitrate, potassium iodide, vitamin C, and GO. Distilled water was used as the solvent. Here, the GO was prepared from natural graphite flakes according to the modified Hummers method similarly to in our earlier reports.[1-5] All chemicals were of analytical grade and used without further purification. In a typical synthesis of the AgI-RGA nanocomposites, the required amount of GO (i.e., 1–5 mg·mL^{-1}) was mixed with 10 mL of DI water and sonicated for 30 min to generate a clear brown dispersion. Then, 0.05 M silver nitrate and potassium iodide were added to the above suspension. Finally, a quantitative amount of vitamin C (0.1 g) was added and uniformly mixed, and the suspension was vigorously sonicated for another 15 min to obtain a homogeneous suspension. Then, the suspension was left undisturbed and unstirred in a muffle furnace at 80 °C for 5 h. The resultant hydrogels were first purified in a large amount of distilled water for at least a week in order to wash out low molecular weight components of the system including excess vitamin C and its oxidized product dehydroascorbic acid [6-8]. Finally, the purified hydrogels were freeze-dried for about 24 h to ensure complete removal of water molecules. AgI samples with different amounts of GO were prepared following the same method with 1, 2, 3, 4, and 5 mg·mL^{-1} of GO (referred to as AgI-1, AgI-2, AgI-3, AgI-4, and AgI-5, respectively). The synthetic process is illustrated in Fig. S1(a). The corresponding digital images of the AgI-reduced graphene oxide hydrogels are shown in Fig. S1(b). From these images, it is clearly evident that the water in which the hydrogels were suspended was completely transparent and clear, which suggests that the entire composite was self-assembled and incorporated into the hydrogel. To synthesize the AgI nanostructures, 0.05 M silver nitrate and potassium iodide were dispersed in 10 mL of DI water, and the mixture was stirred for 15 min. Finally, the resulting precipitate was washed several times with DI water before being dried in air at 60 °C.

The morphologies and average particle sizes were measured using a Hitachi S-4800 field emission scanning electron microscope (FESEM) equipped with an Inca 400 energy-dispersive spectrometer from Oxford Instruments. The microstructure properties were measured using a JEOL JEM-2100F transmission electron microscope (TEM) with an accelerating voltage of 200 kV. Phase determination of the as-prepared powders was performed using a Bruker D8 Advance X-ray diffractometer with a Cu Kα X-ray source. X-ray photoelectron spectroscopy (XPS) was performed using a monochromated Al Kα X-ray source (hν = 1486.6 eV) at an energy of 15 kV/150 W. Raman spectra were obtained on a Nanofinder 30 micro-Raman spectrometer with a solid-state laser (excitation at 487.55 nm) at room temperature in the range of 500–2500 cm^{-1}. Fourier-transform infrared (FTIR) spectra were recorded between 4000 and 500 cm^{-1} at a spectral resolution of 4 cm^{-1} using a Nicolet 380 FTIR spectrometer. The optical absorption measurements were performed using a Shimadzu UV-1800 double-beam spectrophotometer. Photoluminescence (PL) measurements were performed at room temperature using an Hitachi F-7000 fluorescence spectrophotometer. The nitrogen adsorption–desorption isotherm measurements for the samples were carried out at 77.35 K using a Tristar 3000 Micromeritics instrument to measure the surface area and porosity. Prior to adsorption the samples were out-gassed for 3 h under vacuum at 200°C.

The photocatalytic abilities of the AgI and AgI-RGA nanocomposites were evaluated via the degradation of RhB under simulated solar irradiation and visible light irradiation. A solar simulator equipped with an AM 1.5G filter and 150 W Xe lamp (Abet Technologies) was used as the light source. To generate only visible light, a long pass filter ($\lambda \geq 430$ nm) was used. For photocatalysis analysis, the photocatalyst (100 mg) was suspended in a 100 mL aqueous solution of RhB (C_o = 10 mg·L^{-1}). At given time intervals of illumination, 2 mL aliquots of the mixture were removed and centrifuged at 5000 rpm for 15 min to separate the photocatalyst powder. After centrifugation, the UV-visible spectra of the supernatants were recorded to monitor the degradation behaviour. The characteristic absorption peak of RhB at 554 nm was used to assess the extent of degradation. The mineralization ratio of RhB solution was determined by total organic carbon (TOC) value which was obtained by a TOC analyzer (TOC-VCPH, Shimadzu, Japan). In addition, for an in-depth understanding of the role of the photogenerated radical species in the photocatalytic degradation of RhB over AgI-2 nanocomposite, a series of controlled experiments were further performed using 2-Na EDTA, Tert-butyl alcohol and benzoquinone as scavengers of h^+, $\cdot OH$, and $\bullet O_2^-$. The proton NMR spectra were obtained by Varian Mercury Plus 300 MHz and 600 MHz spectrometer in $CDCl_3$ using tetramethylsilane as an internal reference.

Photo-electrochemical measurements were performed in a three-electrode system using a CHI708C electrochemical workstation. A solar simulator equipped with an AM 1.5G filter and 150 W Xe lamp (Abet Technologies) was used as the irradiation source to produce monochromatic illuminating light. The reference and counter electrodes were a Ag/AgCl and platinum wire, respectively, and Na_2SO_4 aqueous solution served as the electrolyte. To prepare the working electrode, the as-synthesized AgI and AgI-2 nanocomposites were first dispersed into ultra-pure DI water using soft ultrasonic stirring to obtain a uniform suspension. The solution containing the catalyst was dropped onto the pretreated indium–tin oxide (ITO) conductor glass substrate, which was then dried in an oven at 100 °C for 3 h. Photo-responses were measured at 0.0 V during on-off cycling of the solar simulator. Electrochemical impedance spectroscopy (EIS) was carried out at open-circuit potential over the frequency range of 10^5 and 10^{-1} Hz with an AC voltage magnitude of 5 mV.

The as-synthesized AgI and AgI-RGA nanocomposites in the presence of $NaBH_4$ were adopted as a reaction for the catalytic reduction of 4-nitrophenol. In a typical procedure, 0.7 ml aqueous solutions of $NaBH_4$ (0.04 M) and 1.7 ml of 4-nitrophenol (0.1 mM) were mixed with ultra-pure water and stirred until the solution turned from light yellow to deep yellow; at this point, the as-synthesized catalyst (70 mg) was added. The reduction rate of 4-nitrophenol was monitored via UV-visible spectroscopy at specific time intervals.

2-Methyl indole (2 mmol), aldehyde (1 mmol), and AgI-2 nanocatalyst (10 mg) were added to a conical flask and stirred vigorously at 70 °C. The progress of the reaction was monitored using thin layer chromatography (TLC). After completion of the reaction, the reaction mixture was extracted with chloroform. All the isolated reaction products were characterized and confirmed by ^1H and ^{13}C NMR spectroscopy using a Varian Mercury Plus 300 MHz and 600 MHz spectrometer in $CDCl_3$ using tetramethylsilane as an internal reference.

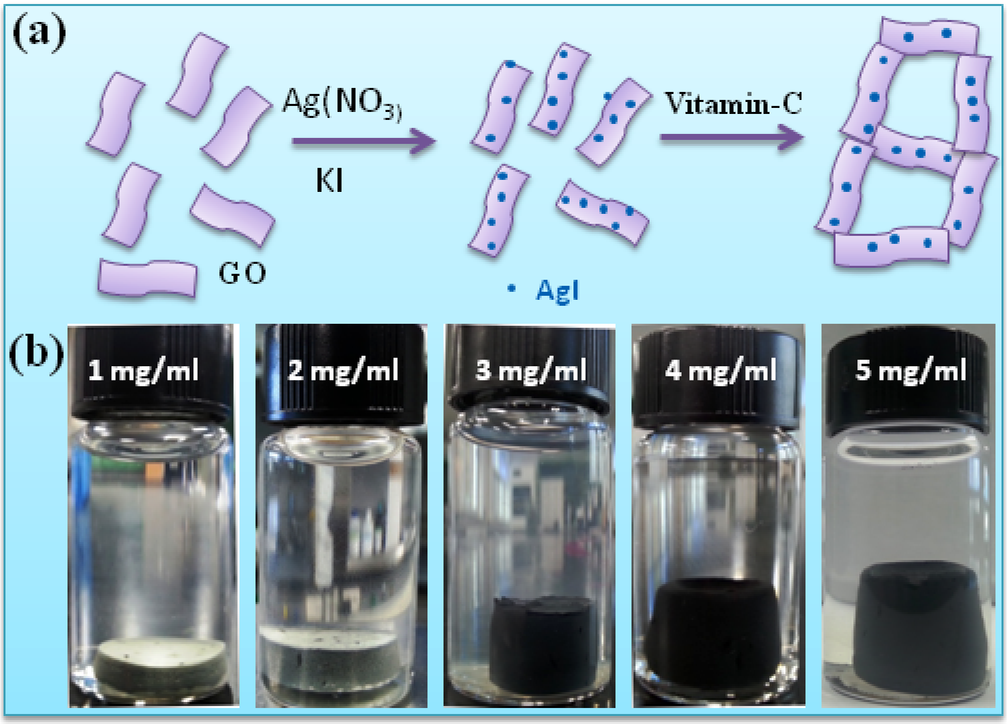

Fig. S1: (a) Schematic diagram of the mechanism of formation of AgI-reduced graphene oxide hydrogel (b) Digital photos of the AgI- reduced graphene oxide hydrogels with different concentrations of GO.

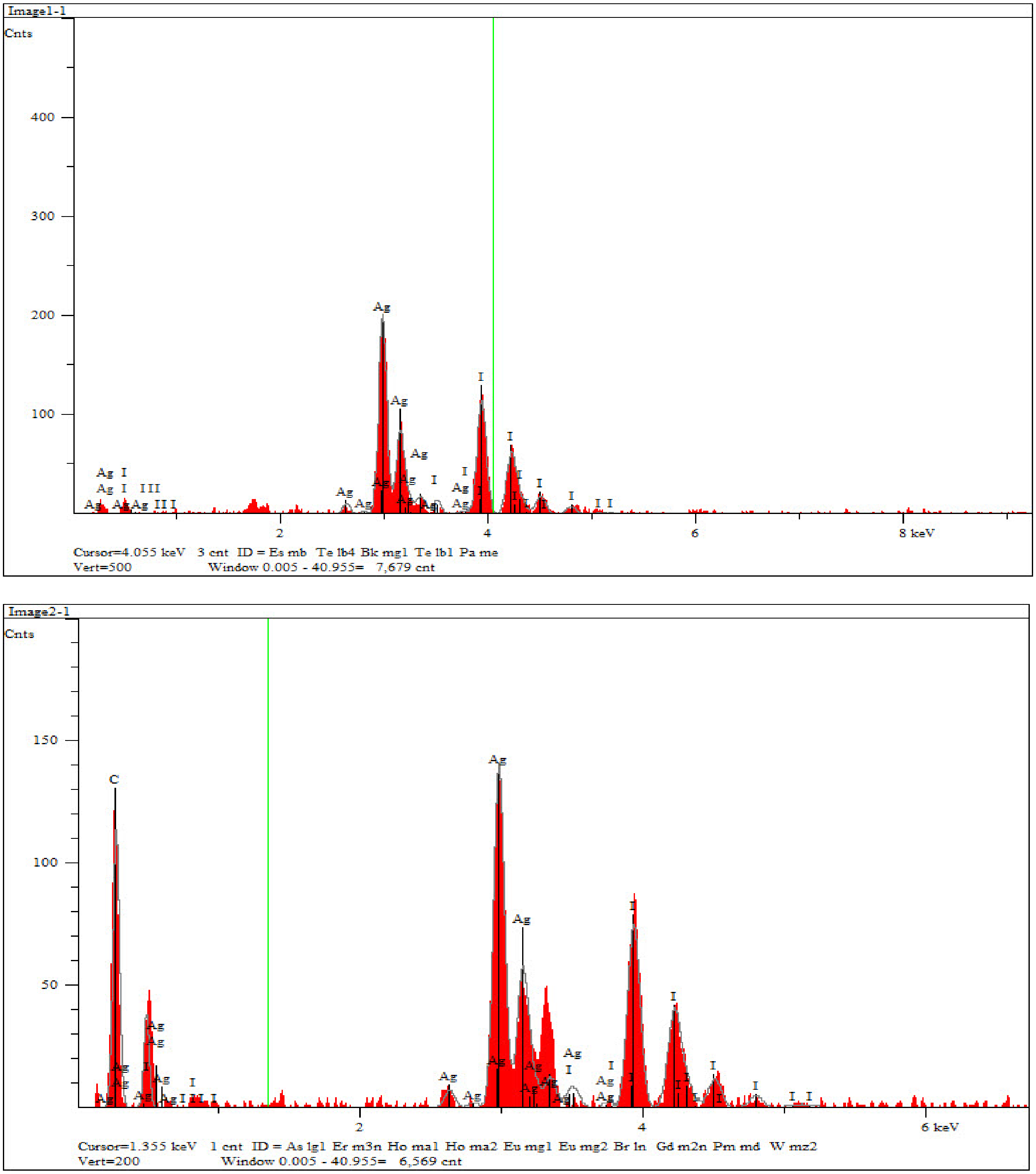

Fig.S2: EDS spectra of (a) AgI and (b) AgI-2 reduced graphene oxide aerogel nanocomposites.

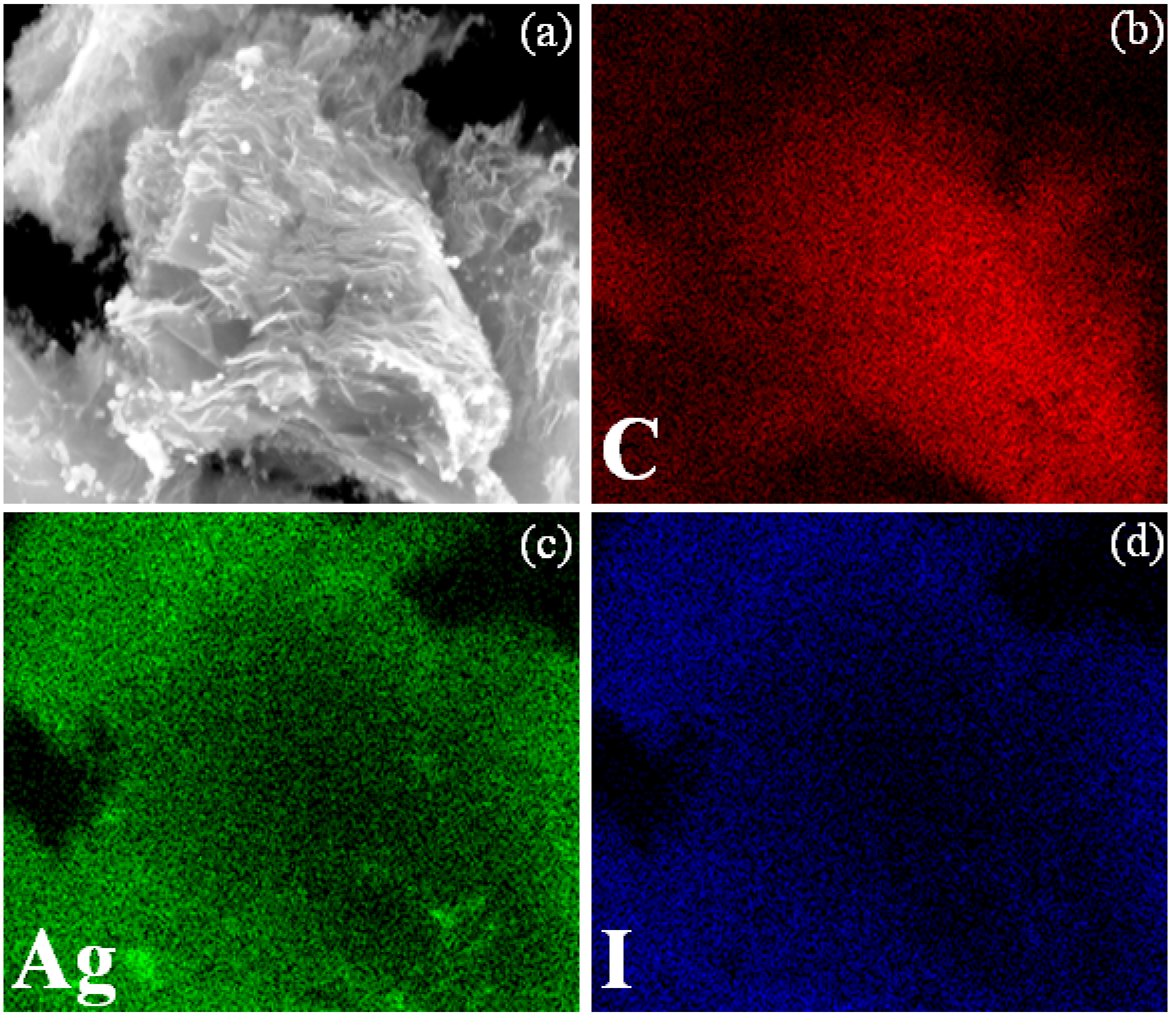

Fig.S3: (a) Electron micrograph and elemental mapping of AgI-3 sample showing the presence of (b) C (c) Ag and (d) I elements, respectively.

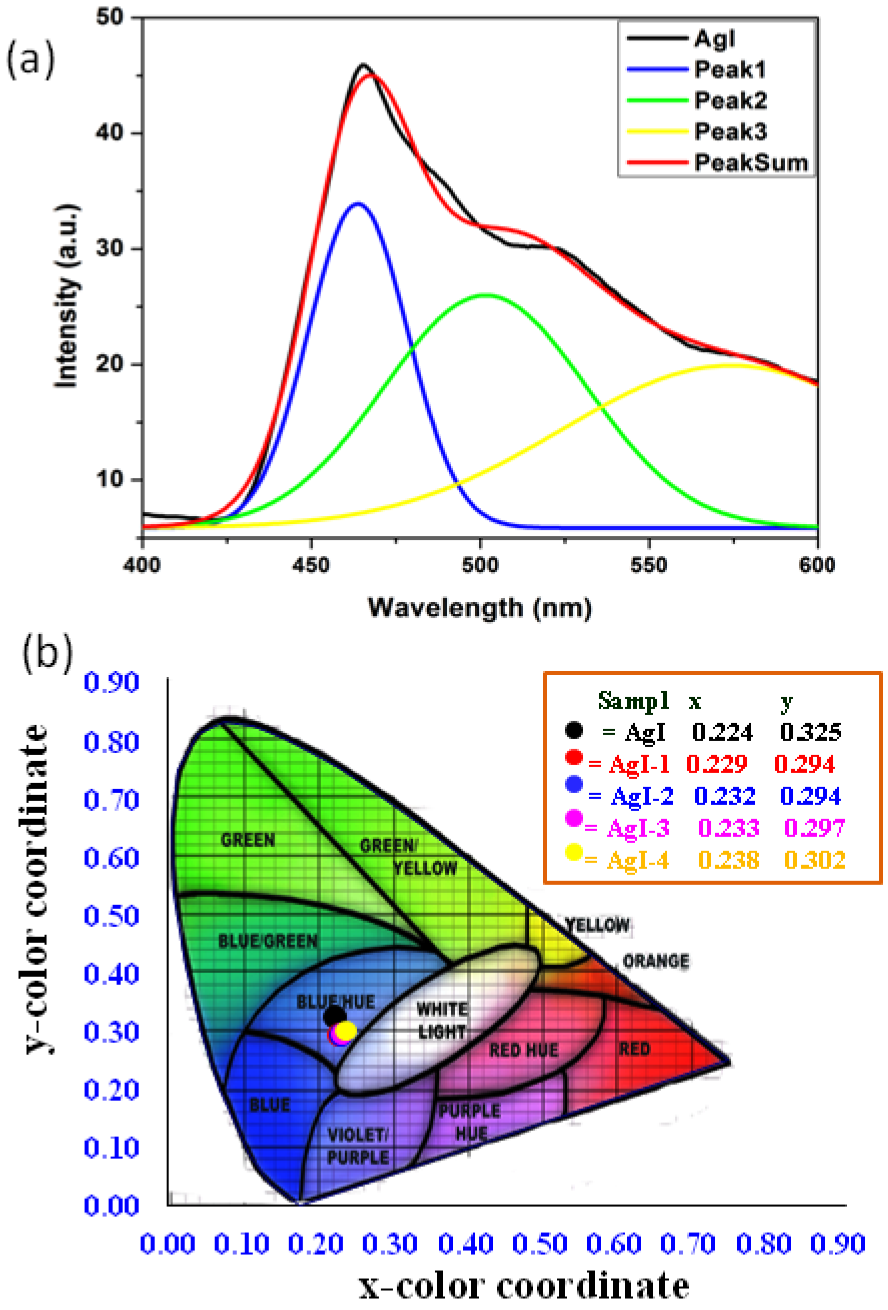

Fig.S4: (a) Gaussian-fit of PL data for pure AgI nanostructures. (b) The estimated CIE chromaticity coordinates of synthesized nanocomposite in the blue-hue region.

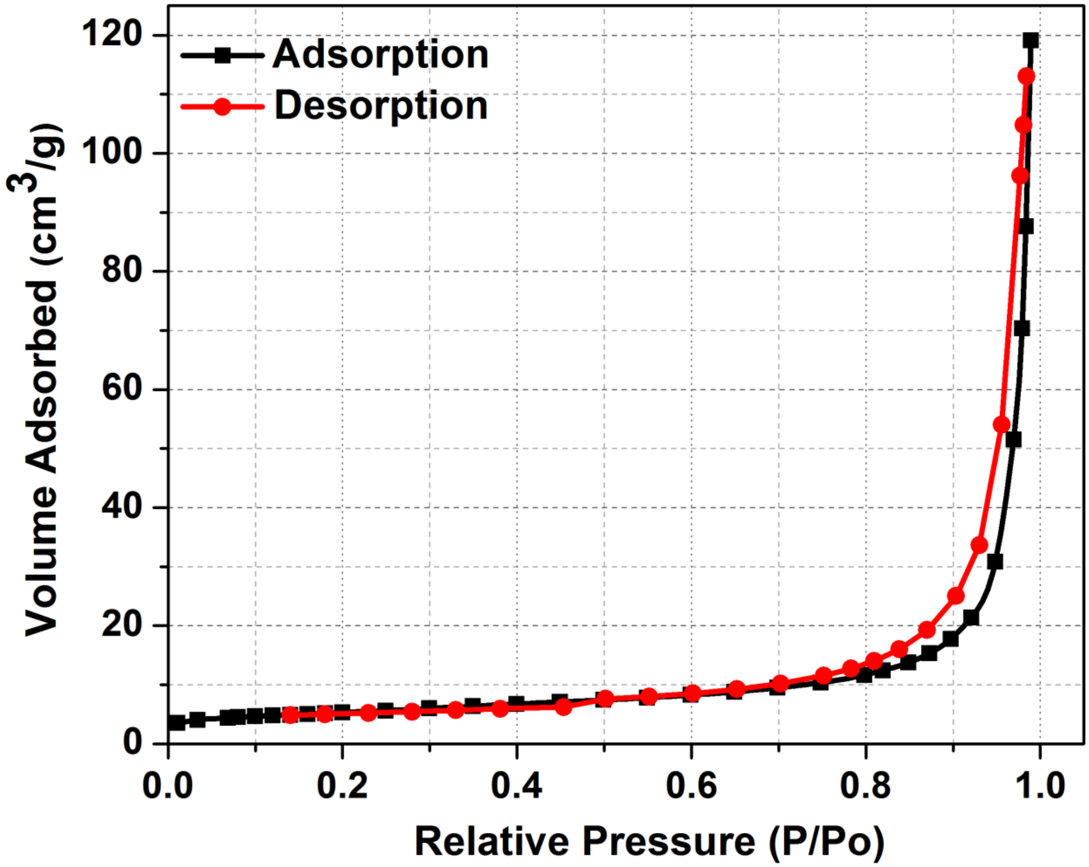

Fig. S5: Nitrogen adsorption–desorption isotherms of AgI-2 nanocomposite.

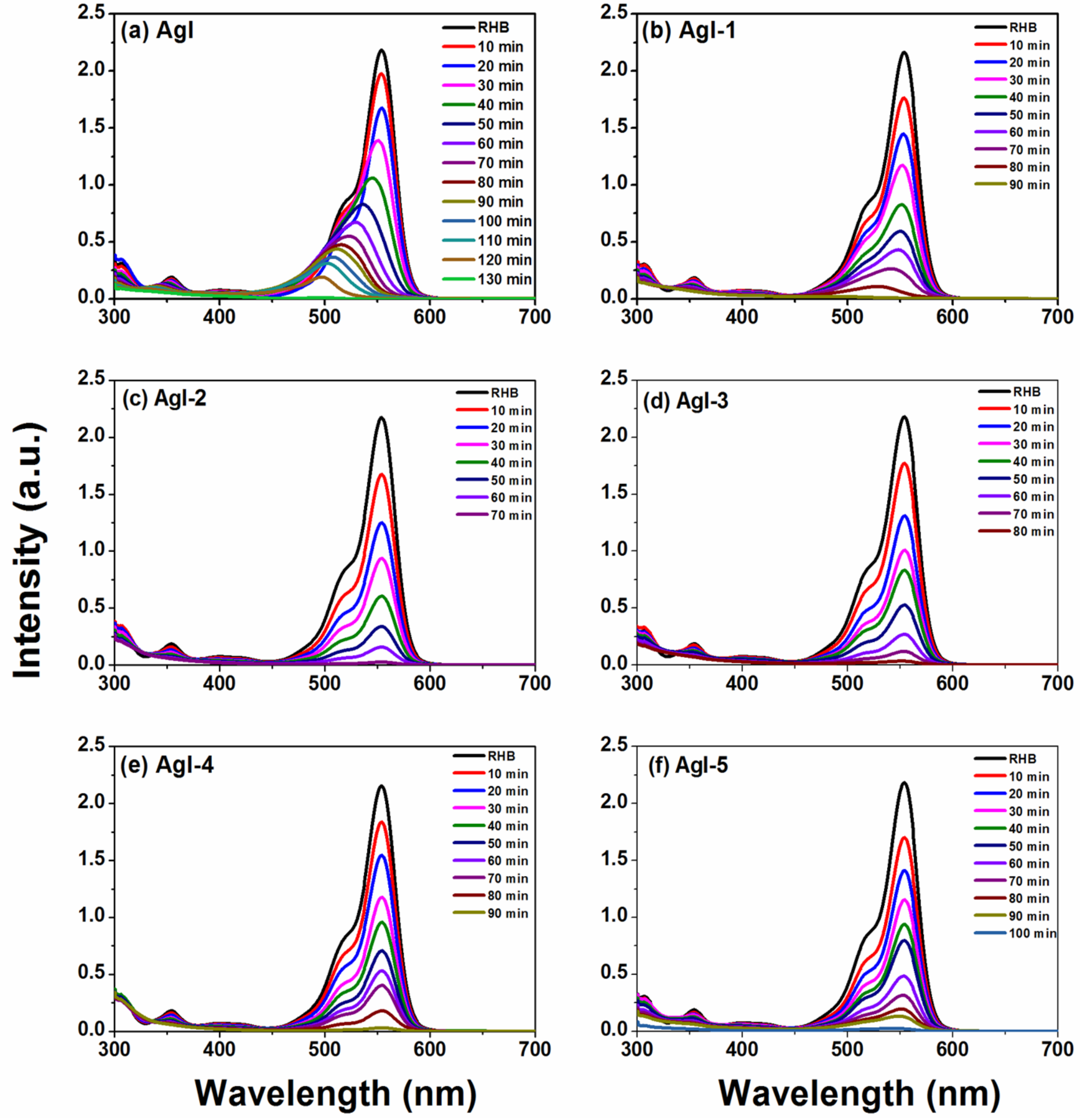

Fig. S6: Changes in the UV-vis absorption spectra of RhB aqueous solution in the presence of (a) AgI, (b) AgI-1 (c) AgI-2, (d) AgI-3, (e) AgI-4 and (d) AgI-5 nanocomposites.

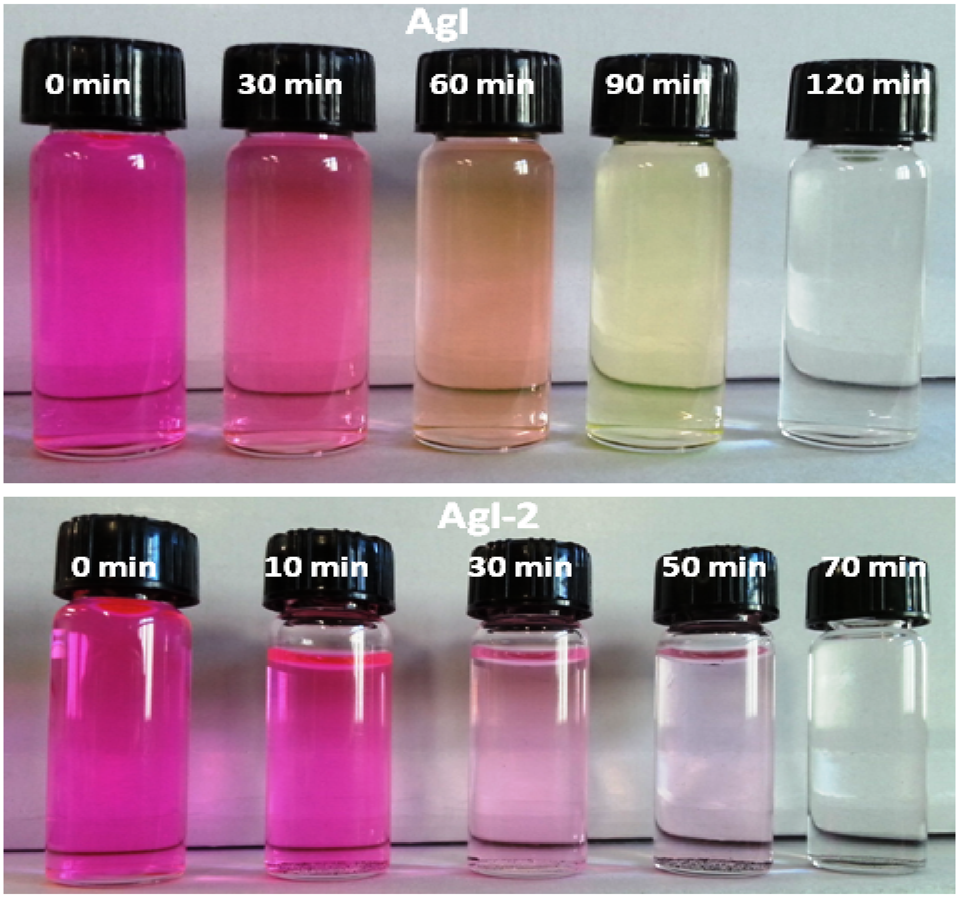

Fig. S7: Aliquots indicating the color change at different time intervals during the degradation of RhB in the presence of (a) AgI and (b) AgI-2 reduced graphene oxide aerogel nanocomposite under simulated sun light irradiation.

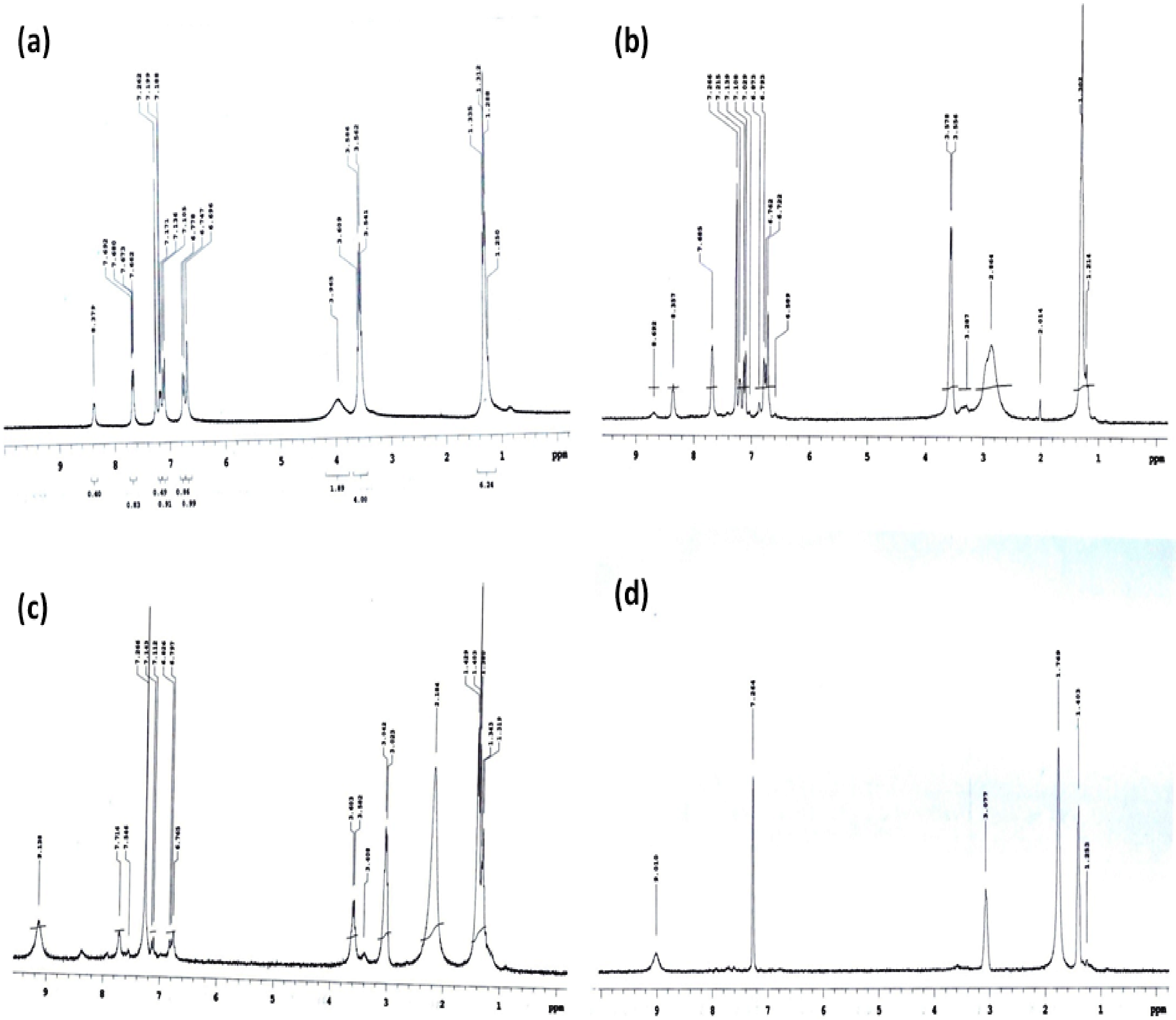

Fig. S8: Proton NMR spectral profiles of the changes occurring during the degradation of RhB at different irradiation times (a) 0 min, (b) 30 min (c) 90 min and (d) 120 min in the presence of AgI nanostructures.

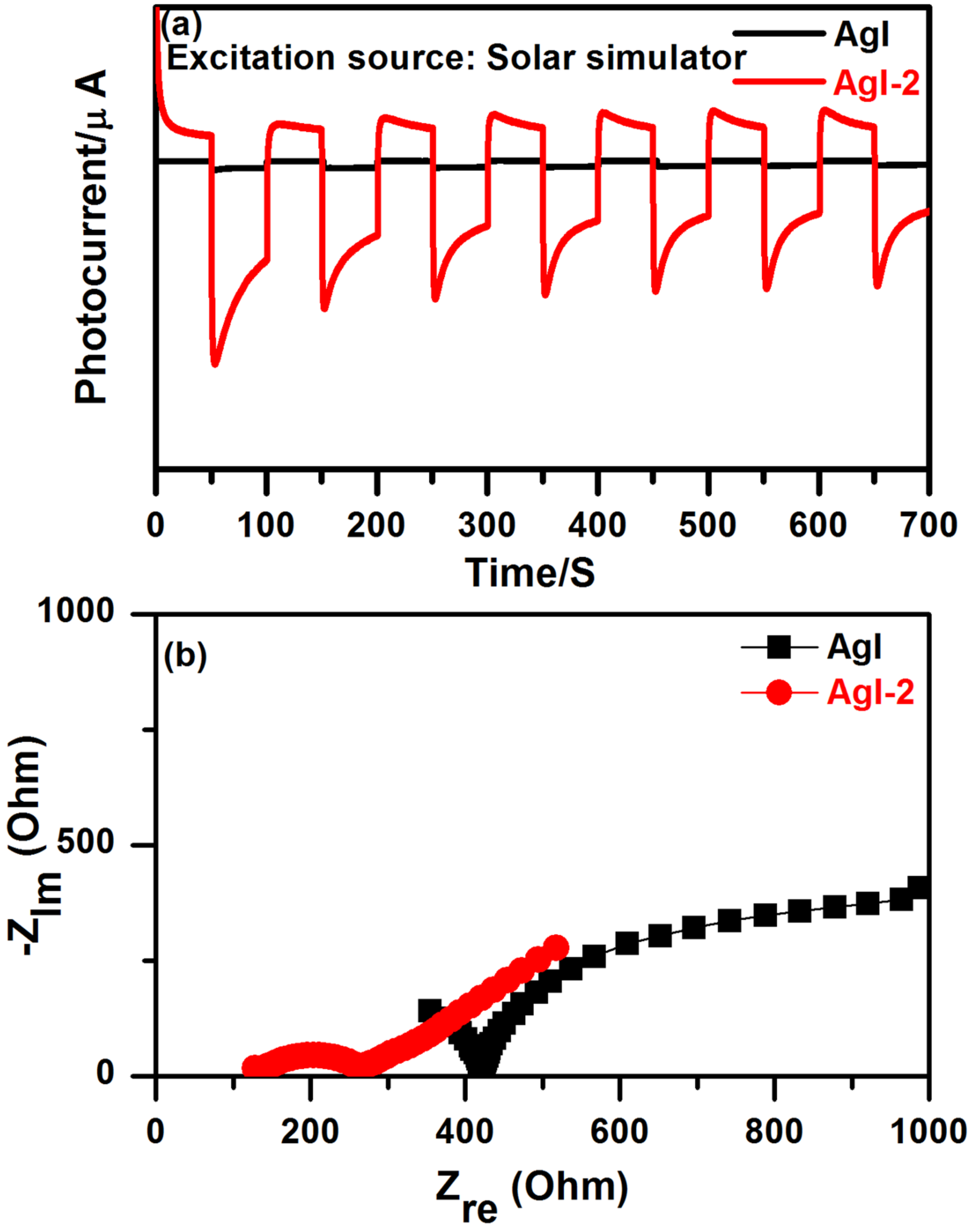

Fig. S9: (a) Transient photocurrent responses of the pure AgI and AgI-2 nanocomposite (b) Electrochemical impedance spectroscopy (EIS) Nyquist impedance plots of the sample electrodes of AgI and AgI-2 nanocomposites.

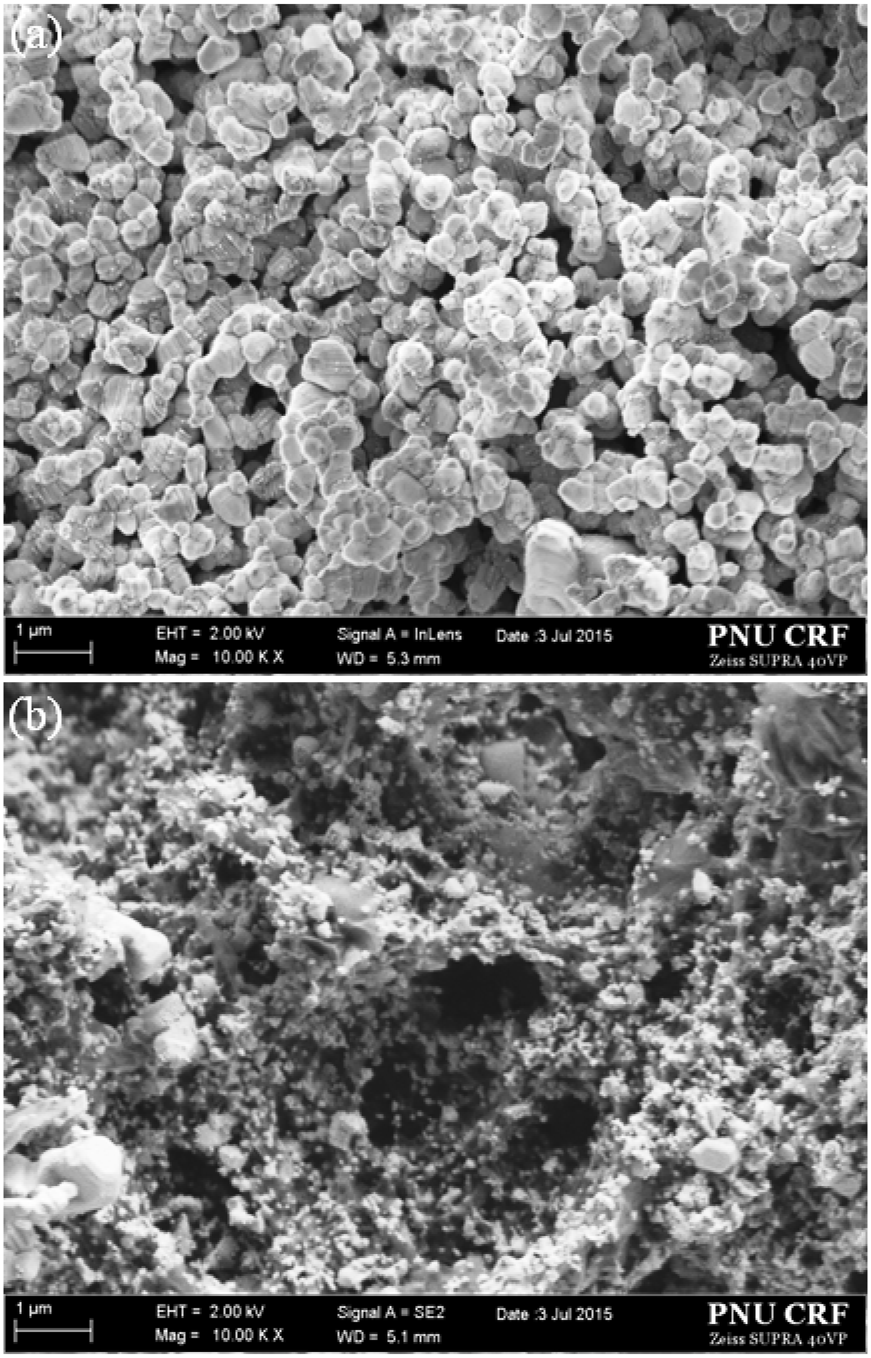

Fig. S10: FESEM images of (a) AgI (b) AgI-2 nanocomposites after five runs under the simulated sunlight irradiation for the degradation of RHB.

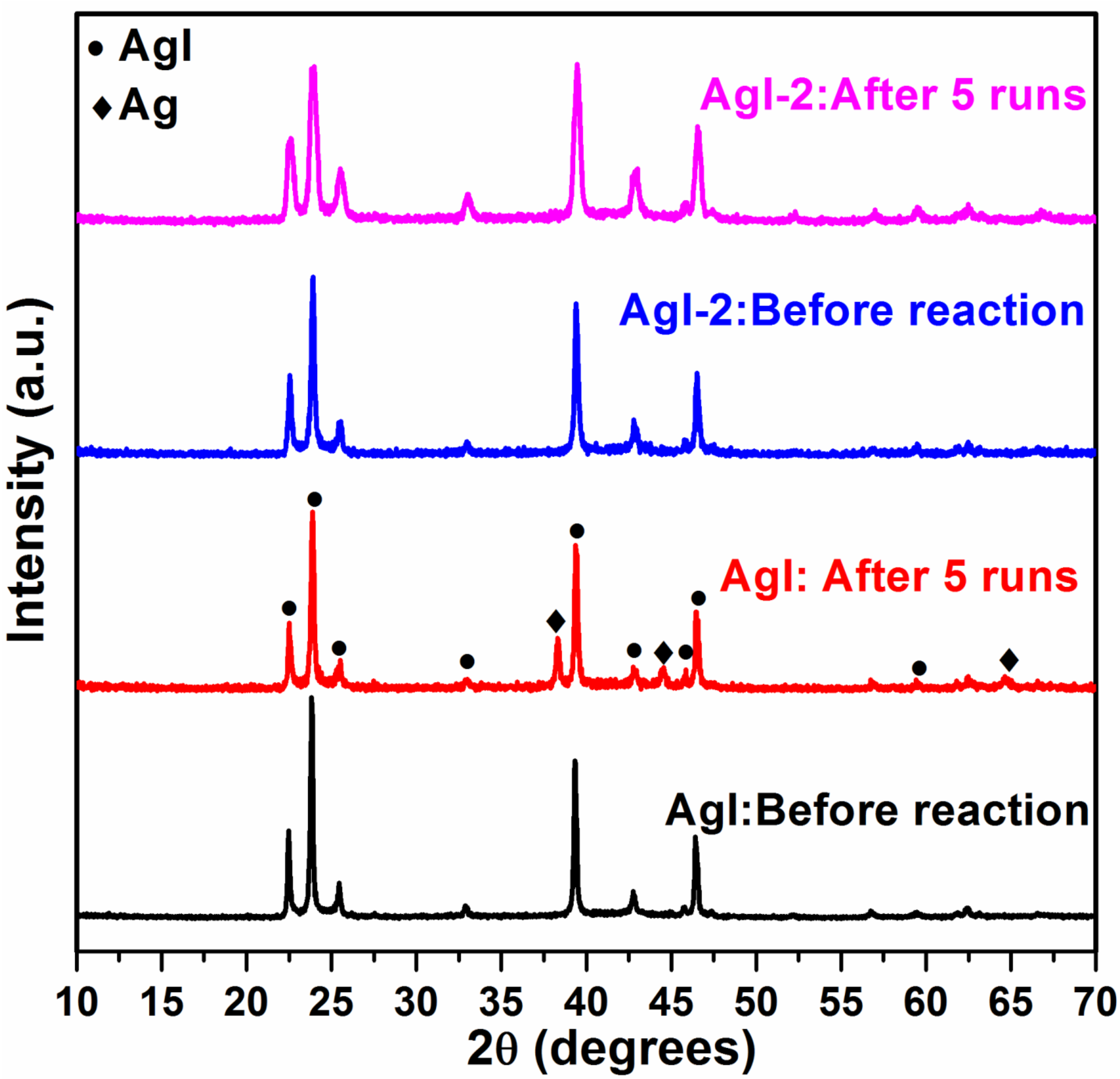

Fig.S11: XRD patterns of AgI and AgI-2 nanocomposite before and after five runs.

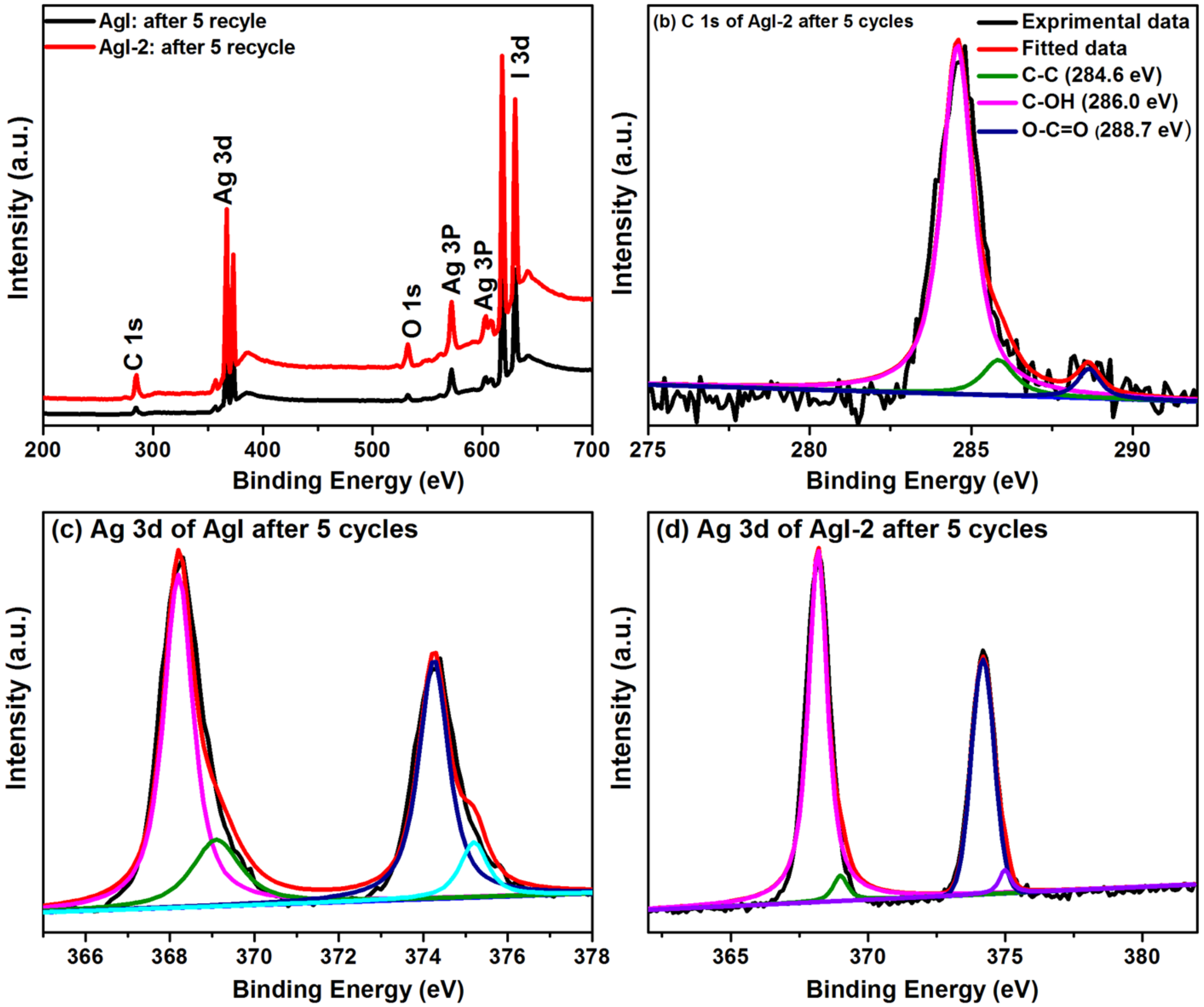

Fig.S12: (a) XPS survey spectrum of AgI and AgI-2 nanocomposites after five runs under the simulated sunlight irradiation for the degradation of RHB. (b) Narrow scan C 1s spectrum of AgI-2 nanocomposites (c) and (d) narrow scan Ag 3D spectra of AgI and AgI-2 nanocomposite.

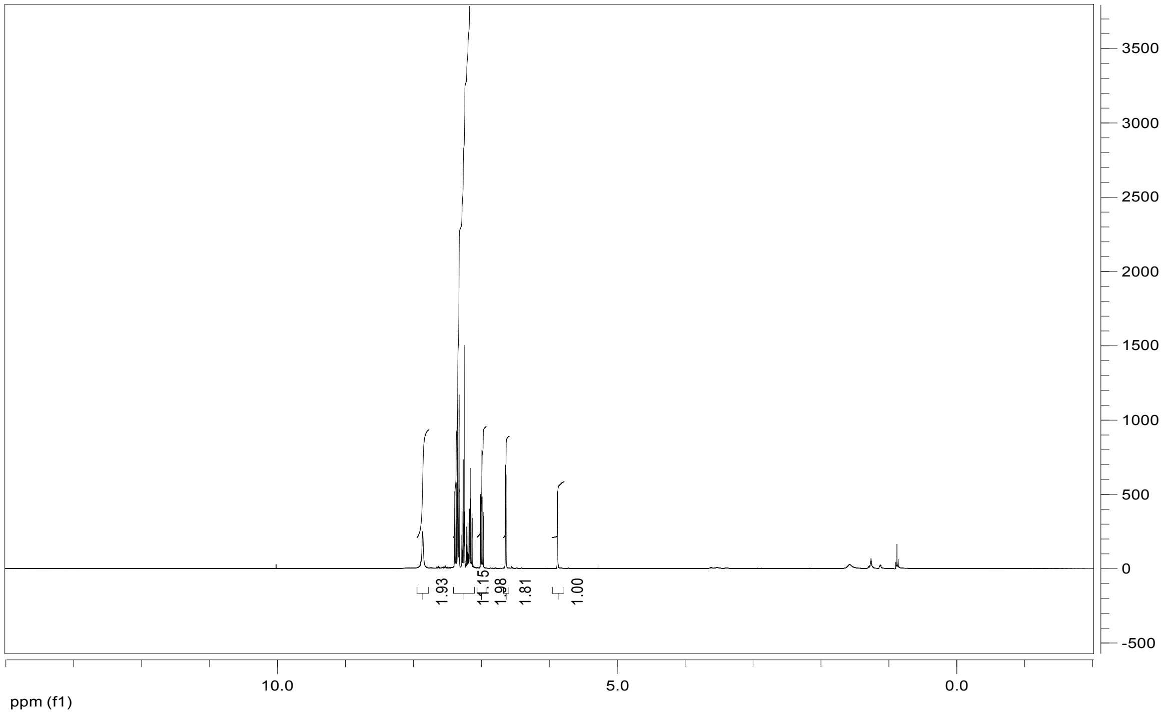

3500
3000
2500
2000
1500
1000
500
0
-500
1.93
11.15
1.98
1.81
1.00
10.0
5.0
0.0
ppm (f1)

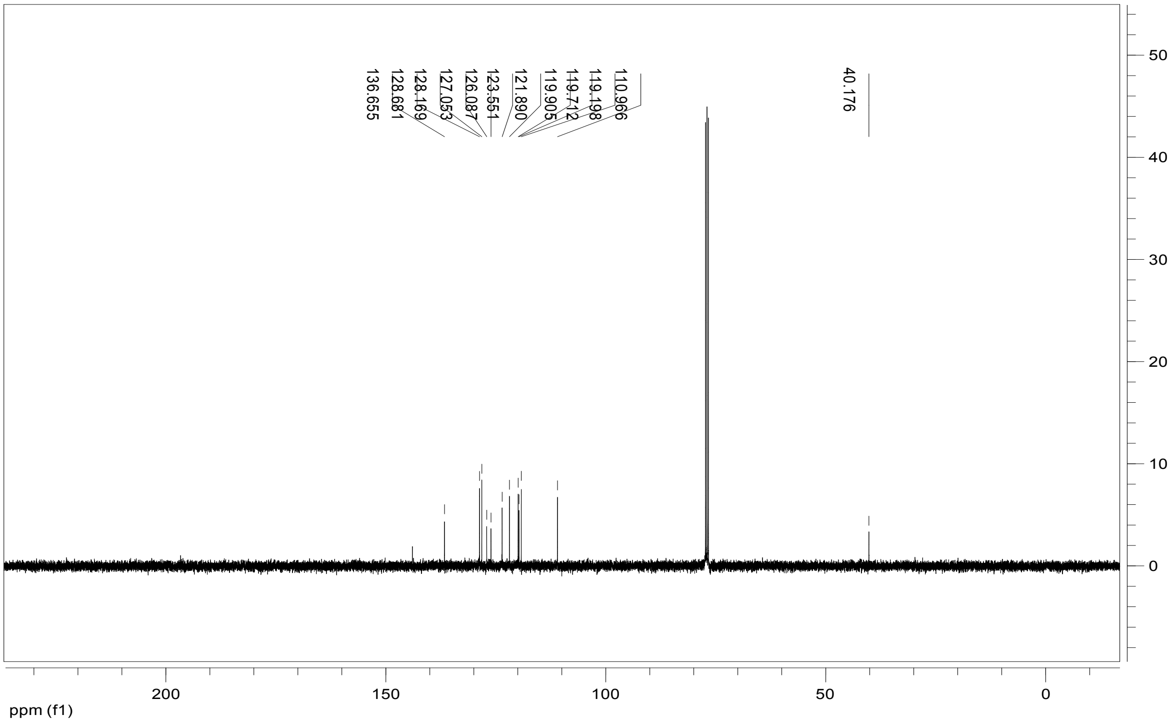

136.655
128.681
128.169
127.053
126.087
123.551
121.890
119.905
119.712
119.198
110.966
40.176
50
40
30
20
10
0
200
150
100
50
0
ppm (f1)

Fig.S13: ^{1}H and ^{13}CNMR spectra of the bis(indolyl) methane resultant compound.

Reaction condition and characterization of AgI-2 nanocomposite
85% yield in 25 min reaction time; solid, 13C NMR (100 MHz, $CDCl_3$): δ(ppm) 144.62, 136.91, 129.72, 128.73, 126.82, 126.31, 125.90, 123.91, 122.02, 121.13, 119.22, 111.41, 40.71. 1H NMR (300 MHz, $CDCl_3$): δ(ppm) 10.07 (s, 2H, –NH), 8.26–6.92 (m, 13H, Ar–H), 6.56 (s, 2H, =CH), 5.93 (s, 1H,Ar–CH) [9].

References:

[1] D. C. Marcano, D.V. Kosynkin, J. M. Berlin, A. Sinitskii, Z. Sun, A. Slesarev, Lawrence B. Alemany, W. Lu, J. M. Tour, ACS Nano, 2010, 4, 4806-4814.

[2] D.A. Reddy, J. Choi, S. Lee, R. Ma, T.K. Kim, RSC Adv., 2015, 5, 18342–18351.

[3] D.A. Reddy, R. Ma, M.Y. Choi, T.K. Kim, Appl. Surf. Sci., 2015, 324, 725–735.

[4] D. A. Reddy, S. Lee, J. Choi, S. Park, R. Ma, H. Yang, T.K. Kim, Appl. Surf. Sci., 2015, 341, 175–184.

[5] D. A. Reddy, R. Ma, T. K. Kim, Ceram. Int., 2015, 41, 6999–7009.

[6] Z. Sui, Q. Meng, X. Zhang, R. Ma, B. Cao, J. Mater. Chem., 2012, 22, 8767–8771.

[7] W. Chen, L. Yan, Nanoscale, 2011, 3, 3132–3137.

[8] X. Zhang, Z. Sui, B. Xu, S. Yue, Y. Luo, W. Zhan, B. Liu, J. Mater. Chem., 2011, 21, 6494–6497.

[9] K.R. Naidu, S.I. M. Khalivulla, P.C. R. Kumar, O. Lasekan, Org. Commun. 2012, 5, 150-159.